# CRITICAL DEFECTS IN DIFFERENT SINTER HARDENING GRADE STEELS TESTED UNDER GIGACYCLE FATIGUE LOADING

**M. Dlapka, H. Danninger, C. Gierl, B. Weiss, G. Khatibi, A. Betzwar-Kotas**

***Abstract***
*Ultrasonic resonance fatigue testing with 20 kHz frequency enables a very fast testing of different materials up to very high loading cycle numbers, 1 billion cycles taking only 15 hours; this method is also extremely sensitive to larger defects. Therefore it is a perfect tool for investigating the critical defects responsible for failure.*
*In the present study different sinter hardening grade steels alloyed with Cr and Mo/Ni were tested up to $10^9$ cycles. It turned out that Cr alloy steels show superior fatigue endurance strength but are more sensitive to intergranular failure initiation compared to Mo/Ni and Cu based ones. The reason for this difference caused by the alloying system can be explained by the high tendency to form brittle grain boundary carbides for Cr low alloyed steels.*
***Keywords: sinter hardening, ultrasonic resonance fatigue testing, Astaloy CrM, intergranular failure***

## INTRODUCTION

Sinter hardening is a heat treating method that has gained more and more importance for PM steel components in the last decades [1]. Therefore a high number of different materials are available on the market. Newer ones mainly contain Cr or Mn as alloying elements which are very attractive in terms of costs and performance if the parts manufacturers are able to provide proper sintering. If this is not the case, Ni and Mo containing variants are still attractive alternatives, despite the cost penalty.

Especially for automotive applications for which the price challenges are extremely tough, sinter hardening is the most cost effective way to obtain high strength materials, for example for engine or transmission applications [2]. Especially such automotive components should provide high fatigue resistance, because a failure might have dramatic consequences. Some of these parts are loaded up to extremely high cycle numbers. In the last years it became clearer that something like a fatigue endurance limit, as used for a long time in literature and practice, does not exist in reality [3]. Even when going to very high cycle numbers ($>10^7$) failure still appears. For Al and austenitic steels this has been well known for a long time, but for other systems, e.g. steels, the concept of a real endurance limit is still used frequently.

Therefore a good knowledge of these ultra high cycle fatigue regions is essential for the understanding of the material behaviour and the possibly appearing critical defects in this regime, in order to improve the material properties for such applications.

Magdalena Dlapka, Herbert Danninger, Christian Gierl, Vienna University of Technology, Institute for Chemical Technologies and Analytics, Vienna, Austria
Brigitte Weiss, Golta Khatibi, Agnieszka Betzwar-Kotas, University of Vienna, Faculty of Physics, Department of Physics of Nanostructured Materials, Vienna, Austria

The problem when testing to very high cycle numbers is that with conventional testing systems this is extremely time consuming or simply impossible (testing up to $10^{10}$ cycles will take 320 years for a conventional system operating at 1 Hz, and still 8 years at 40 Hz). Therefore in this case ultrasonic resonance fatigue testing with 20 kHz testing frequency is a highly attractive alternative because it allows a testing up to $10^{10}$ cycles within 7 days and up to $10^9$ even within 15 hours [4, 5, 6].

In the present work, different sinter hardening materials were tested, containing Cr or Mo/Ni and Cu as alloying elements. They were tested using the described ultrasonic resonance fatigue testing system up to $10^9$ cycle numbers as a "runout criterion". These materials were Höganäs AB powder grades Astaloy CrM+0.5%C with and without 1%Ni, and Distaloy LH (0.9%Mo/0.9%Ni)+0.5%C+1%Ni. The fatigue behaviour was tested and the fracture surfaces were investigated in detail to be able to draw conclusions which are the most critical defects in sinter hardened steels loaded to extremely high cycle numbers.

## EXPERIMENTAL DETAILS

### Sample Preparation

Four different sinter hardening steel grades were tested containing different alloying elements. Some were mainly alloyed with chromium; others contained significant amounts of Mo/Ni and Cu. The four different materials tested are listed in Table 1. The preparation was done by uniaxial die pressing to bars with ~30x~12x~120 mm and sintering at 1120 or 1250 °C in $N_2$-10%$H_2$ for 60 min.

Tab.1. Composition of the different sinter hardening materials tested.

| | In base material | | | | admixed | | |
|---|---|---|---|---|---|---|---|
| | Cr [wt.%] | Mo [wt.%] | Ni [wt.%] | Cu [wt.%] | C [wt.%] | Ni [wt.%] | Cu [wt.%] |
| A: Distaloy LH | - | 0.9 | 0.9 | 2 | 0.5 | 1 | - |
| B: Astaloy CrM | 3 | 0.5 | - | - | 0.5 | - | - |
| C: Astaloy CrM +Ni | 3 | 0.5 | - | - | 0.5 | 1 | - |

The length of the fatigue test specimen was calculated according to equation 1. This was possible after measuring the acoustic (dynamic) Young's modulus (Equation 2) (ASTM E1876). Young's modulus was measured using a resonance system. There, samples are excited to resonance by an impulse (impact with a hammer). The resulting vibration, which depends on the properties of the tested material, is detected. The modulus is calculated via equation 2.

$$L = \frac{1}{2f} \cdot \sqrt{\frac{E}{\rho}}$$

Equation 1: Calculation of the resonant bar length

$$E = 4 f^2 l^2 \rho$$

Equation 2: Calculation of the acoustic (dynamic) Young's Modulus

L…specimen length [m]; f…measured frequency [Hz], E…dynamic Young's Modulus [Pa], ρ…sintered density [kg/m³], l…specimen thickness [mm]

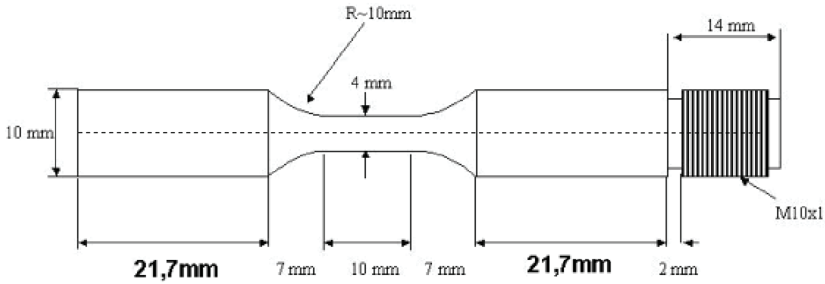


Fig.1. Testing geometry for Astaloy CrM + 0.5%C +1 %C sintered at 1250°C and sinter hardened from 1120°C separately.

For the shaping (turning) the samples were soft annealed. After surface finishing, which included grinding (with grinding paper) and polishing with $Cr_2O_3$ paste, the specimens were reheated to 1120°C and sinter hardened from this temperature with a cooling rate of ~1.5 K/s. This means that the samples actually were double sintered; the 1250°C specimens were only sintered at this temperature but hardened from 1120°C. There were no residual stresses present at the surface on the finished specimen because the reheating to 1120°C resulted in a complete relaxation of the compressive residual stresses present after shaping and surface finishing, and the relative mild gas quenching did not result in any measurable resudial stresses.

Tab.2. Measured dynamic E-modulus for different sintering temperatures and the calculated shoulder length.

| | 1120°C | 1250°C | 1120°C | 1250°C |
|---|---|---|---|---|
| Material composition | E-Moduli | | Shoulder length | |
| A (DLH+1%Ni+0.5%C) | 150 | 167 | 18.5 | 20.2 |
| B (Astaloy CrM+0.5%C) | 164 | 176 | 21 | 21.2 |
| C (Astaloy CrM+1%Ni-0.5%C) | 171 | 181 | 22 | 21.7 |

**Fatigue testing**

The fatigue tests were performed in push-pull mode at ~20 kHz. The testing system consists of an ultrasonic generator with a control unit, followed by a transducer. The transducer is connected to an acoustic horn and a coupling piece. The sample was fixed on the coupling piece. A strain gauge was fixed on the coupling piece for controlling the actual strains. A circulating cooling system was used for keeping the specimen and the coupling piece at room temperature and inhibiting corrosion at the same time (Fig.2); otherwise at this high frequency damping effects would result in rapid heating of the specimens, with resulting uncontrollable change of the mechanical properties.

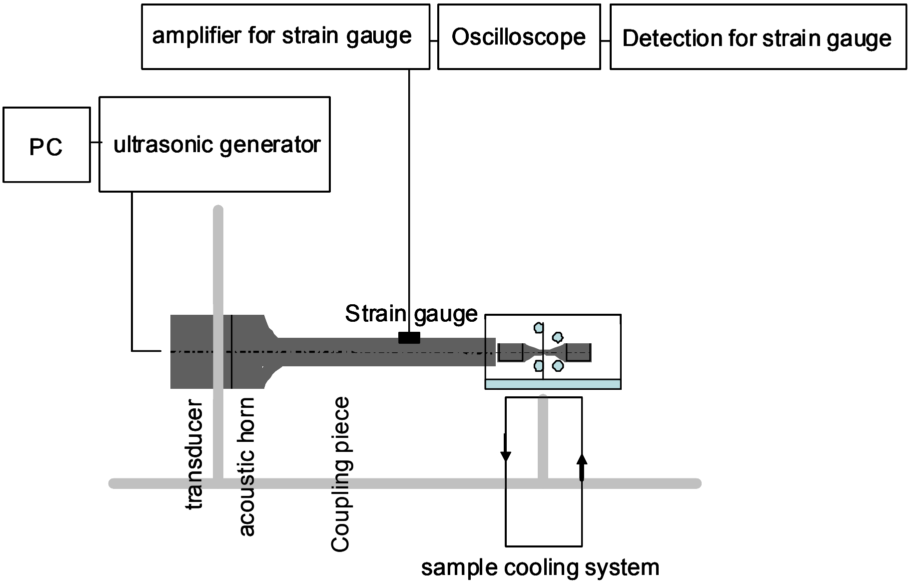


Fig.2. Equipment for the ultrasonic fatigue testing (schematic).

**Calibration**

Compared to conventional fatigue testing systems, for which measurement of the applied load is easily possible using a load cell, the stress calibration for the gigacycle fatigue tester is much more complicated since the load cannot be recorded directly nor can the strain be measured directly on the specimen during testing. The tester thus has to be calibrated for each material. For the calibration one strain gauge was fixed on a sample and one on the coupling piece. The resulting strain values in correlation with the applied excitation amplitude (indicated on the resonance generator) were recorded. During the real fatigue tests, the signals from the strain gauge at the coupling piece were continuously recorded. With the help of the strain values and the E-moduli of the different materials it was possible to calculate the resulting stress for a given excitation amplitude. For the calculation of the S-N curves this stress correlated to the amplitude from the calibration was used.

## RESULTS

**S-N-curves**

The obtained S-N-curves are shown in Fig.3 and Fig.4. It is obvious that higher sintering temperature resulted in higher stress values, especially for the Astaloy CrM based materials. The reason is the reduction of the oxides which is not complete after sintering at 1120°C while 1250°C results in full reduction of the oxides [7, 8]. This is also the reason why the CrM is superior compared to the Distaloy LH at 1250°C while the values are rather similar for the lower sintering temperature. This means that if the full potential of the Astaloy CrM should be used, sintering at high temperature, e.g. 1250°C, is absolutely necessary.

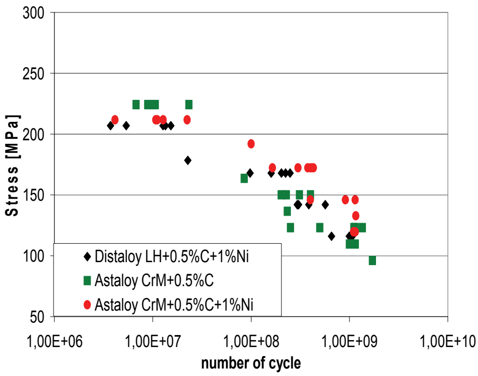


Fig.3. S-N-curves for different sinter hardening materials, sintering temperature 1120°C.

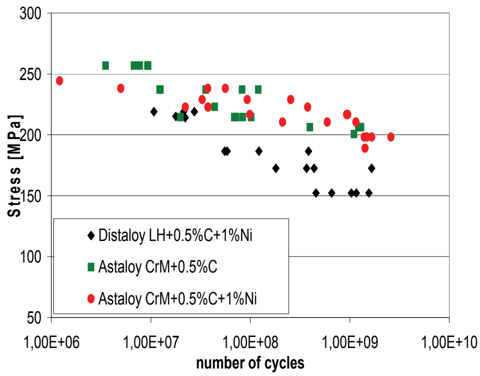


Fig.4. S-N-curves for different sinter hardening materials, sintering temperature 1250°C.

The fracture surfaces of the tested specimen were investigated. As the fracture surface contained significant amounts of pores it was rather difficult to identify the initiating area only by SEM. Therefore a combination of photos taken with a digicam, a stereomicroscope and a SEM were used. This way the starting zone could be found for almost all specimens.

**Fracture surfaces**

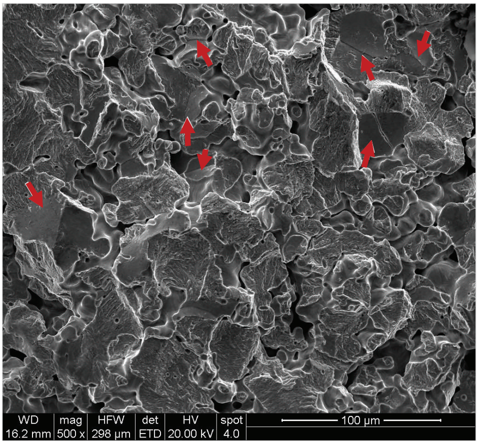


Fig.5. Distaloy LH+0.5%C+1%Ni sinter hardened at 1120°C.

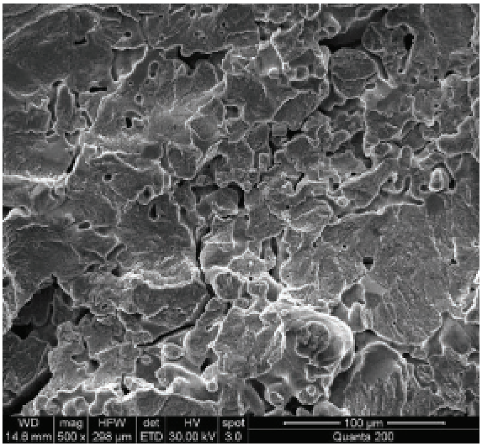


Fig.6. Distaloy LH+0.5%C+1%Ni sinter hardened at 1250°C.

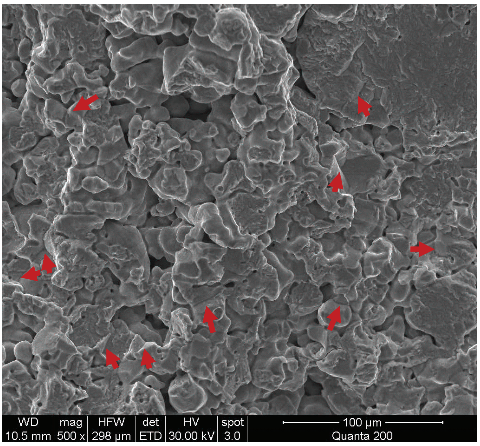


Fig.7. Astaloy CrM+0.5%C sinter hardened at 1120°C.

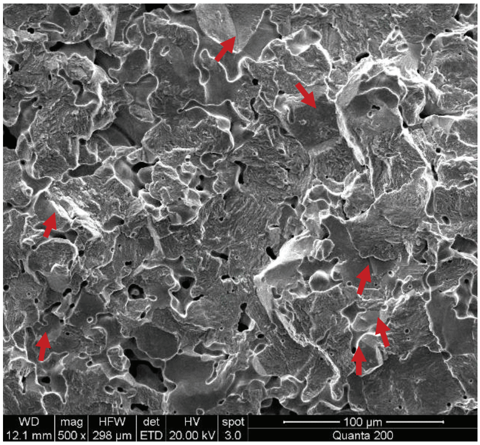


Fig.8. Astaloy CrM+0.5%C sinter hardened at 1250°C.

All the appearing fracture surfaces were dominated by transgranular failure, which is typical for martensitic structures, as expected for sinter hardened materials which should be completely martensitic. Beside this, regions of intergranular failure were found, mainly for the Astaloy CrM materials especially after sintering at 1120°C (Fig.7). At this lower sintering temperature also for Distaloy LH some intergranular failure was found (Fig.5), but significantly lower amounts than for the Cr containing Astaloy CrM. This material was furthermore investigated with 1% Ni additionally. For this composition the amount of intergranular failure increased even further (Fig.9).

Astaloy CrM+0.5%C+0%Ni

Astaloy CrM+0.5%C+1%Ni

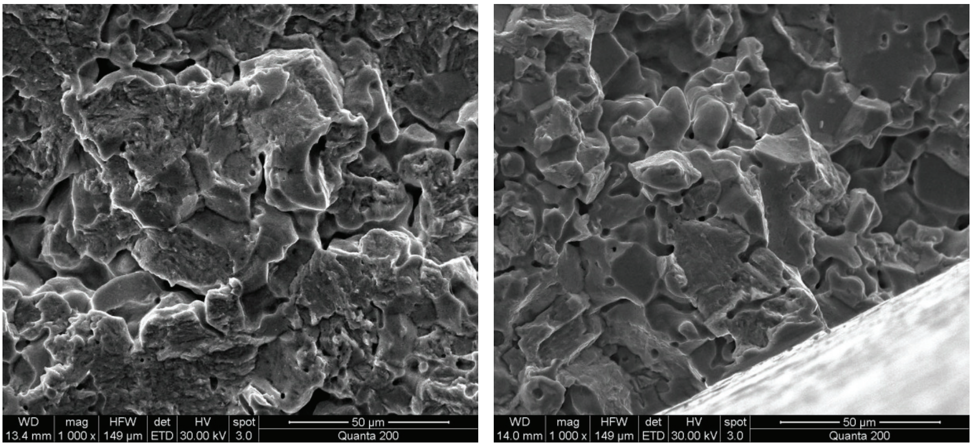


Fig.9. Intergranular failure of Astaloy CrM+0.5%C with and without carbon addition.

**Intergranular failure**

As mentioned above, there were considerable areas of intergranular failure present in the Cr alloyed sinter hardened materials (Astaloy CrM+0.5%C, Astaloy CrM+1%Ni+0.5%). A possible reason for this is the fact that Cr as alloying element is shifting the eutectoid point to the left [9]. This means that even smaller amounts of carbon compared to the system Fe-C cause the formation of cementite, which might be present here as film-like cementite at the grain boundaries. Of course film-like precipitates on the grain boundaries can cause a dramatic weakening of these areas, and therefore the crack goes through these boundaries without any marked resistance.

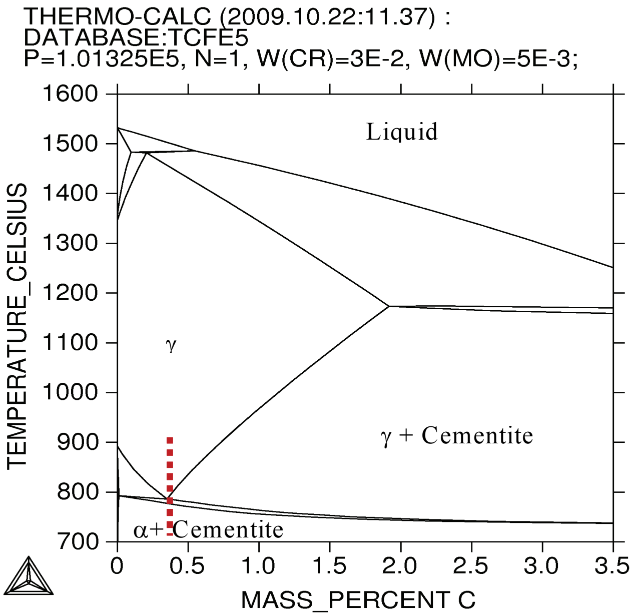


Fig.10. Phase diagram for Astaloy CrM+x%C, red line marks the eutectoid composition. [9]

It was found that the highest amounts of intergranular failure were present in the system Astaloy CrM. In Distaloy LH based material, only for the lower sinter hardening temperature some intergranular failure was found, due to the absence of the shifting Cr, and the content of the - also shifting Mo - is much lower here. Sintering at higher temperatures resulted in lower amounts of cementite. The reason is the lower amount of carbon after sintering at 1250°C due to the more effective carbothermal reduction at this temperature, causing a higher carbon loss for the same starting levels compared to 1120°C and therefore in less tendency to form cementite. Moreover it was seen that adding Ni (material C compared to material B) resulted in higher amounts of cementite. This means that Ni is an element increasing the sensitivity to the formation of brittle cementite phases by shifting the eutectoid point a little bit further to the left. The reason is that Ni increases the carbon activity and furthermore is not forming carbides itself. This means that the tendency to form cementite is increased [10].

Another reason might be the appearance of graphite agglomerates in the material which might result in too high carbon contents near these large C particles. One argument for this hypothesis is the combination of large pores (the carbon is dissolved during sintering, leaving a pore behind) and intergranular nests which were found frequently. Carbon is diffusing pretty fast in the matrix, but if the material is just at the border to cementite formation even small differences might have a pronounced effect (Fig.11).

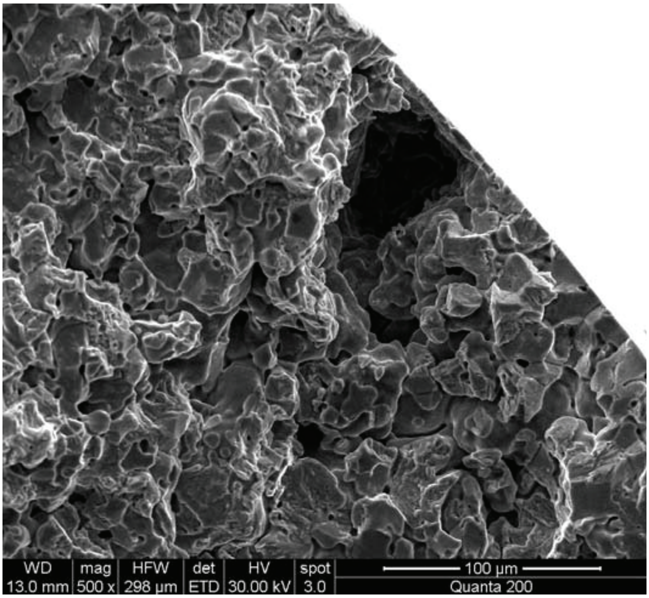


Fig.11. Large pore linked to intergranular failure located at the surface.

However a final proof of this hypothesis of cementite at the grain boundaries is extremely difficult because measuring carbon in film-like thickness with extremely high lateral resolution is a tough analytical topic. One possible method would be Auger electron spectrometry (AES) analysis, but there the samples should exhibit fresh surfaces, e.g. by breaking in ultrahigh vacuum. The surfaces of interest here were however obtained by ultrasonic resonance fatigue testing using a liquid cooling with anti-corrosion agents as an additive in the solution. This additive is of course based on organic compounds. Therefore the surfaces of the specimens were contaminated by organic deposits immediately upon fracture. Therefore the AES analyses did not result in any useful result.

An alternative explanation would be the presence of oxides at the grain boundaries. This would also explain the higher amounts of intergranular failure when sinter hardening at lower temperatures. The level of the oxygen content was however as expected for the Astaloy CrM after sintering at 1250°C and therefore no oxidation of the material was indicated. Anyway the formation of cementite is more likely since the amount of oxygen in the material was quite low; furthermore, previous studies on Astaloy CrM [7, 8] have shown that the surface oxides, which are most detrimental for interparticle bonding, are usually removed already when sintering at 1120°C, at least in reasonably oxygen-free atmosphere. Also the percentage of sulphur was extremely low, indicating that the formation of sulphides at the grain boundaries is very unlikely. Anyway the amount of combined carbon was surprisingly high for a material with 0.5%C admixed (usually ~0.35%C would be expected after sintering at 1250 °C). This seems to be one of the main aims for this intergranular failure appearing in the fracture surfaces.

Tab.3. Elemental analysis after sintering at 1250°C and then sinter hardened from 1120°C.

| | C [%] | O [%] | S [%] |
|---|---|---|---|
| Astaloy CrM+0.5%C Sinter hardened | 0.470+0.006 | 0.013+0.002 | 0.0013+0.0004 |

## CONCLUSIONS

In the present work sinter hardening materials were investigated via ultrahigh cycle fatigue testing up to 10E9 cycles. Astaloy CrM turned out to be superior in terms of fatigue but only after sintering at higher temperatures (1250°C) due to the incomplete carbothermal reduction at lower temperatures.

The fracture surfaces were dominantly transgranular which is typical for martensitic materials, but especially the Astaloy CrM contained significant amounts of intergranular failure, which means that the material was suffering embrittlement. The most likely explanation for this is the formation of film like cementite at the grain boundaries due to the shifting of the eutectoid point to the left by the present amounts of Cr. This makes the material highly sensitive to the carbon content, since if the amount is above the eutectoid point the formation of cementite is possible and therefore also an embrittlement of the material. If Ni is present the material is even more sensitive to the admixed amount of carbon. This means that a precise carbon control is absolutely vital to obtain good fatigue properties for the Astaloy CrM.

**Acknowledgement**

The authors would like to thank Höganäs AB, especially Sven Bengtsson and Björn Lindqvist, for the funding of Höganäs Chair round IV.

## REFERENCES

[1] Yu, Y. In: Proc. PM Asia. April 2007, Shanghai, China
[2] Ratzi, R., Orth, P. In: Proc. Society of Automotive Engineers. Detroit 2000, p. 129
[3] Sonsino, CM.: Konstruktion, vol. 57, 2005, p. 87
[4] Weiss, B., Stickler, R.: Modern Developments in Powder Metallurgy, vol. 21, 1988, p. 3
[5] Danninger, H., Weiss, B.: Powder Metallurgy Progress, vol. 1, 2001, no. 1
[6] Spoljaric, D., Danninger, H., Weiss, B., Chen, DL. In: Proc. DF PM'96 Int. Conf. Deformation and Fracture in Structural PM Materials. Vol. 1. High Tatras, Slovakia, 1996, p. 147
[7] Kremel, S., Danninger, H., Yu, Y.: Powder Metallurgy Progress, vol. 2, 2002, no. 4, p. 211
[8] Campos, M., Kremel, S., Marcu Puscas, T. In: Proc. European Conference on Powder Metallurgy. Nice, 2000, p. 47
[9] Castro, F., Ortiz, P. In: Proc. European Conference on Powder Metallurgy. Vol. 1. Nice, 2003, p. 261
[10] Bocchini, GF.: Powder Metallurgy Progress, vol. 4, 2004, no.1